Spatial Variation of the Foil Parameters from in Situ Calibration of the JT-60U Imaging Bolometer Foil

Homaira P. ARAGHY, Byron J. PETERSON, Hiromi HAYASHI, Shigeru KONOSHIMA[1)], Naoko ASHIKAWA, Dongcheol SEO[2)] and the JT-60U TEAM[1)]

National Institute for Fusion Science, Toki, Gifu 509-5292, Japan
[1)]*Japan Atomic Energy Agency, Naka, Ibaraki 311-0193 Japan*
[2)]*National Fusion Research Center, Yuseong, Daejeon 305-806, Korea*

(Received 7 December 2006 / Accepted 20 April 2007)

We obtained the local foil properties of the JT-60U imaging bolometer foil (a single graphite-coated gold foil with an effective area of $9 \times 7\,\mathrm{cm}^2$ and a nominal thickness of $2.5\,\mu\mathrm{m}$) such as the thermal diffusivity, κ, and the product of the thermal conductivity, k, and the thickness, t_f, by calibrating some parts of the foil. Calibration of the foil was made in situ using a He-Ne laser (~27 mW) as a known radiation source to heat the foil. The thermal images of the foil are provided by an infrared (IR) camera (microbolometer type). The parameters are determined by finite element modeling (FEM) of the foil temperature and comparing the solution to the experimental results. In this work we apply this calibration technique to investigate the spatial variation of the foil parameters. Significant variation in the local temperature rise of the foil due to local heating by the laser beam indicates a spatial variation of the foil parameters κ, k and t_f. This variation is possibly due to nonuniformity in carbon coating and/or the thickness of the foil.

Keywords: calibration, He-Ne laser beam, local temperature, variation of the foil parameters, imaging, bolometer

DOI: 10.1585/pfr.2.S1116

1. Introduction

In the Large Helical Device (LHD) [1–3] the infrared imaging video bolometer (IRVB), using a segmented-absorber was applied to measure the plasma radiation in two dimensions [4, 5]. This concept showed some advantages (not requiring electrical components) of the segmented mask infrared imaging bolometer (SIB) compared to resistive bolometers and it was easy to calibrate the foil for each pixel due to separate channels, and the foil is supported by the strong mask against differences in pressure, however it had some problems such as shadowing of the foil by the mask and losses thermal energy due to thermal contact. Thus, the energy losses in JT-60U due to radiative process are measured, with an infrared imaging video bolometer (IRVB) without using a mask [6–9]. The laser calibration could compensate for the complications of the foil calibration due to the absence of a segmented mask frame.

The calibration technique of the IRVB gives confidence in the measured values of the plasma radiation. In a separate work, the spatial calibration data will be used to produce the bolometer intensity data to be utilized in the tomographic analyses. The local foil properties of the foil such as the thermal diffusivity, κ, and the product of the thermal conductivity, k, and the thickness, t_f, are obtained by foil calibration for one part on the foil when the foil is heated by laser power [10].

Here, the spatial variation of the local foil properties of the JT-60U imaging bolometer foil during an in-situ calibration investigation for various locations on the foil is presented. The parameters depending on the spatial position on the foil are determined by finite element modeling of the foil temperature and comparison to the experimental results.

2. The Single Graphite-Coated Gold Foil

For JT-60U a single graphite-coated gold foil as an absorber of the broadband radiation from the plasma is used. The effective area of the gold foil with a nominal thickness of $2.5\,\mu\mathrm{m}$ is $9 \times 7\,\mathrm{cm}^2$. The IR camera side of the foil is blackened with graphite. The foil with a supporting copper frame is mounted on a port inside of the vacuum vessel collimated by an aperture camera. The infrared (IR) camera (with a tangential view) that is shielded by a 2 cm thickness of soft iron, 1.5 cm of lead and 9 cm of the polyethylene against the effects of magnetic field, gamma particles and neutrons, respectively, is installed outside of the vacuum vessel to provide thermal images of the foil. The laser power is directed to the foil by a gold IR mirror and a beam steerer. The calibration setup, foil view with a small spot from the laser beam and a thermal image from the spot after focusing on one part of the foil are shown in Fig. 1. The

author's e-mail: homi@nifs.ac.jp

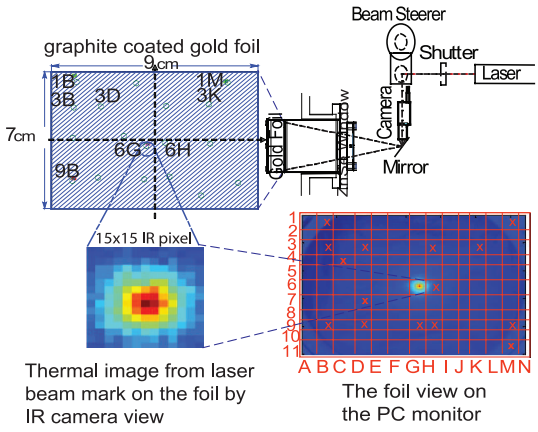

Fig. 1 Drawing of the calibration setup for the IRVB foil calibration of the JT-60U tokamak, foil view with a small spot due to the laser beam effect and a thermal image from the spot after focusing for one part of the foil.

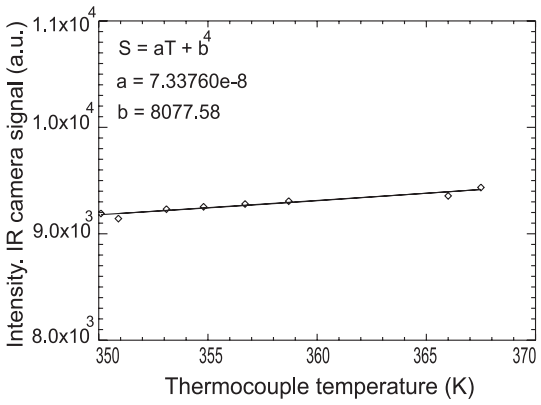

Fig. 2 The results of the IR camera data and plate temperature when they are fit to the Stefan-Boltzmann law to find the calibration coefficients.

foil view by the IR camera is observed on a PC monitor where it is divided into 11×14 sections. The He-Ne laser beam (wavelength of 0.633 μm) is focused on various locations. The thermal images consist of a 15×15 pixel IR view of the foil (~1 cm^2 area of the foil) when the total IR camera pixel number is 168×128. The calibration technique is applied for various positions (1B, 3B,..., 9 M) on the gold foil.

3. Data Analysis Results from the Foil Calibration

The foil calibration is carried out in order to obtain local foil properties to determine the thermal diffusivity, κ, and the product of the thermal conductivity, k, and the thickness, t_f, of the foil. The foil calibration is made through various steps such as determining the location of the laser spot on the foil, and converting the IR thermal radiation data from the IR camera to foil temperature. This is done by using the IR camera calibration when the blackened plate temperature data from a thermocouple and the IR camera data is fit to the Stefan-Boltzmann law [10].

In the previous article [10] the IR camera calibration coefficients a and b had a negligible temperature dependence in the range of temperatures used in the measurement on JT-60U. The calibration factors are corrected to a = 7.34e-8 W/K^4 and b = 8077.58 in the range of experiment temperatures (350-370 K). The resulting IR camera data and plate temperature when they are fit to the Stefan-Boltzmann law to find the calibration coefficients are shown in Fig. 2.

For the foil calibration using a He-Ne laser, the laser power is necessary for solving the heat diffusion equation in two dimensions analytically by using the finite element model (FEM). The laser power is directed into the vacuum chamber through the ZnSe IR window to the foil. The laser transmission power (~27 mW) on various positions of the foil is shown in Table 1.

Table 1 The laser parameters on different positions on the foil of the JT-60U imaging bolometer.

Pixel	Position (pixel)	Position (mm)	Laser power (mW)
9B	(23 , 38)	(-36 , -19)	15.42
3B	(25 , 97)	(-34 , 19)	15.65
1B	(26 , 118)	(-35 , 33)	15.45
3D	(37 , 88)	(-22 , 18)	15.85
6G	(73 , 65)	(-3 , - 2)	16.09
6H	(81 , 66)	(2 , - 1)	15.78
3K	(105 , 88)	(22 , 18)	15.76
1M	(131 , 114)	(31 , 30)	15.61

The laser power decreased after passing through the IR window. By reproducing the calibration on a test stand with a similar ZnSe window the transmission through the ZnSe window could be estimated for each laser position on the foil. The handheld laser power meter is calibrated using a LASERPAD™ PC. The experimental configuration details for eight points on the foil are shown in Table 1.

The spatial variation of the foil parameters κ, k and t_f from in situ calibration of the JT-60U imaging bolometer foil is shown in Fig. 3. The local temperature rise (ΔT) from the foil is shown in Fig. 3 (a). The foil temperature rise was taken from the peak of a 2D Gaussian fitted to the temperature profile from the IR camera. The IR thermal data are averaged over 200 time frames of the steady state data. The FEM is used for solving of the two-dimensional heat diffusion equation (1 in ref. 10) with a constant thickness and thermal parameters of the foil and approximately 2000 spatial points assuming a constant temperature at the foil boundary (frame). The FEM used the measured beam profile, fit to a 2-D Gaussian, as the heat source term. In Fig. 3 (a) a discrepancy between the experimental data with standard deviation (however they are not so obvious) and the modeled data by FEM using the nominal values of t_f

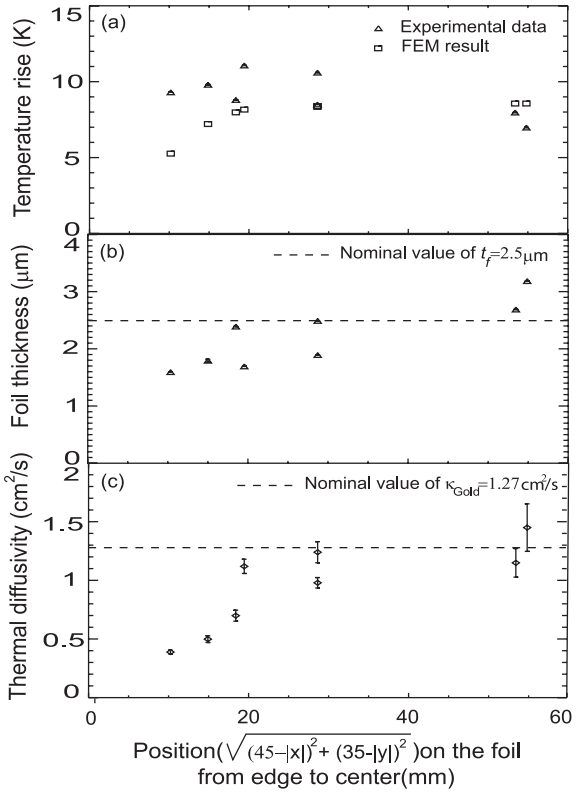

Fig. 3 (a) The foil temperature rise was taken by fitting the temperature profile from the IR camera to a 2D Gaussian. Discrepancy between the experimental data and the modeled data by FEM near the edge has been observed. (b) The spatial variation of t_f. (c) The spatial variation of κ.

and k near the edge has been observed.

The appropriate value of the thickness (t_f) of the foil from the experimental value of the ΔT is found when a second order polynomial is fitted to the kt_f and ΔT data from the FEM (the thermal conductivity (k) is assumed to be constant at the nominal value). The spatial variation of t_f is shown in Fig. 3 (b). The standard deviation was found by propagating the IR camera measurement error through the analysis. However this estimate of the error is less than 0.1 μm. In Fig. 3 (b) a discrepancy between the t_f from various locations with nominal value of the foil thickness (t_f = 2.5 μm) has been observed. These discrepancies decreased from the edge (near the frame) to the center of the foil.

The thermal diffusivity (κ) is also determined by various processes such as fitting the experimental foil temperature data during the decay to the modified exponential equation (2 in ref. 10), fitting the FEM calculation numerical data decay of the foil temperature when the radiation source term in the heat diffusion equation is zero to the modified exponential equation. A second order polynomial is fitted to the κ and τ numerical data from the FEM to find the appropriate value of the thermal diffusivity of the foil from the experimental value of the decay time. The spatial variation of κ with standard deviation is shown in Fig. 3 (c). The discrepancies between the various thermal diffusivities from various locations on the foil with the nominal value of the thermal diffusivity of the foil (κ_{gold} = 1.27 cm^2/s) has been observed. These discrepancies also decreased from the edge to the center of the foil.

4. Discussion

The foil in situ calibration is carried out in order to obtain the local foil properties for the JT-60U tokamak imaging bolometer foil. By comparing the results from the FEM solution to the heat diffusion equation with the experimental values of the foil temperatures and its decays the parameters of the foil are determined for various locations on the foil.

The spatial variation of the foil parameters is obtained by applying this calibration technique to investigate various sections of the foil. Significant variation in the local temperature rise of the foil due to local heating by a laser beam and in its decays indicates a spatial variation of the foil parameters: the thermal diffusivity, the thermal conductivity and the thickness of the foil. One notes that the differences in the factor of kt_f from the expected nominal values for two nearby locations on the foil, for instance 6G and 6H in the center area of the foil, were 10% and 28%, respectively. Also one notes that the experimental local temperature (blackbody radiation) rise data from the edge of the foil near the frame is much higher than the results from the foil center. However, the numerical temperature rise resulting from the FEM near the edge is lower than the results from the center. This discrepancy does not agree with the previous calibration result that was observed [6].

The variation in kt_f and the trend of increasing κ going from the edge to the center are similar to those seen in the previous work (although the standard deviations were not calculated in that case), but the level of κ at the center was higher than the previous case and close to the nominal value. This increase in κ may be due to the diminished effect of the carbon blackening as the foil is 2.5 times thicker in the current case than in the previous work. The discrepancy between the measured temperature rise and the temperature rise predicted by the FEM, in particular at the edge, may be due to improper modeling of the thermal contact between the foil and the frame. In other words, the thermal conduction between the frame and foil may be worse in actuality than the perfect thermal contact assumed by the foil and may also be non-uniform. The obtained thermal diffusivity was also not near to the expected nominal value for gold on some locations, in particular near the edge of the foil. For instance, for the 1B location on the foil near the frame it was 30% of the expected nominal value for gold. However, in the location 6 G near the center it was ~90%. This variation as a function of the proximity to the frame may also be explained by poor thermal contact between the foil and the frame and its improper modeling by the FEM. However, the possibilities also exist that the variation in the foil parameters may depend on some problems

with the IR camera due to possible damage by neutrons and could be related possibly to non-uniformity in the carbon coating and/or the thickness of the foil.

For improving the accuracy of the calibration, we intend to use a new IR camera (SC500) with a resolution of two times more than the previous IR camera (Omega) in a calibration laboratory (low noise environment). By using this new camera with a close-up lens we can image the same area of the foil ($1\,cm^2$) with $\sim 120 \times 120$ pixels instead of the 15×15 pixels used in this case. Also the new IR camera will have 2 times the time resolution, which will improve the exponential fits used to determine κ. In addition, we plan to try blackening the foil with a more uniform graphite coating by using new methods (carbon coating sputtering or glow discharge technique).

Acknowledgment

The authors are grateful to the support given by MEXT Grants–in-Aid #16560729 & #16082207.

[1] O. Motojima *et al.*, Fusion Eng. Des. **20**, 3 (1993).
[2] S. Sudo, J. Plasma Fusion Res. **69** (11), 1349 (1993).
[3] A. Komori *et al.*, Phys. Plasma, **8**, 2002 (2001).
[4] G.A. Wurden, B.J. Peterson and S. Sudo, Rev. Sci. Instrum. **68**, 766 (1997).
[5] B.J. Peterson, Rev. Sci. Instrum. **71**, 3696 (2000).
[6] B.J. Peterson, A. Yu. Kostrioukov, N. Ashikawa, M. Osakabe, and S. Sudo, Rev. Sci. Instrum. **74**, 2040 (2003).
[7] S. Konoshima, B.J. Peterson, N. Ashikawa, Y. Miura, and the JT-60U team, 32th EPS, Tarragona (2005).
[8] H. Parchamy, B.J. Peterson, S. Konoshima, N. Ashikawa, and the JT-60U team, 22th JSPF Conference, Tokyo (2005).
[9] B.J. Peterson, S. Konoshima, H. Parchamy, M. Kaneko, T. Omori, D.C. Seo, N. Ashikawa, A. Sukegawa and the JT-60U Team, J. Nucl. Mater. **363-365**, 412 (2007).
[10] H. Parchamy, B.J. Peterson, S. Konoshima, H. Hayashi, D.C. Seo, N. Ashikawa, and the JT-60U team, Rev. Sci. Instrum. **77**, 515 (2006).